

Reversal of polarization in amidophosphines: neutral- and anionic- κP coordination vs. anionic- $\kappa P, N$ coordination and the formation of nickelaazaphosphiranes

Ingo Schranz,^a Graham R. Lief,^a Christopher J. Carrow,^a Dana C. Haagenson,^a Luke Grocholl,^a Lothar Stahl,^{*a} Richard J. Staples,^b Ramamoorthy Boomishankar^c and Alexander Steiner^c

^a Department of Chemistry, University of North Dakota, Grand Forks, ND, 58202-9024, USA.
E-mail: lstahl@chem.und.edu

^b Department of Chemistry and Chemical Biology, Harvard University, Cambridge, MA, 02138, USA

^c Department of Chemistry, University of Liverpool, Liverpool, UK L69 7ZD

Received 18th May 2005, Accepted 22nd July 2005
First published as an Advance Article on the web 16th August 2005

Nickel(II) chloride reacts with the bis(*tert*-butylamino)diazadiphosphetidine $\{\text{Bu}^t(\text{H})\text{NP}(\mu\text{-NBu}^t)_2\text{PN}(\text{H})\text{Bu}^t\}$ to form *trans*- $[\{\text{Bu}^t(\text{H})\text{NP}(\mu\text{-NBu}^t)_2\text{PN}(\text{H})\text{Bu}^t\}_2\text{NiCl}_2]$. In solution and the solid-state each heterocyclic ligand coordinates nickel through one phosphorus atom only. For comparison the solid-state structure of the known *trans*- $[\text{NiCl}_2(\text{PEt}_3)_2]$ was also determined and it was found that the two complexes have almost identical bond parameters about nickel. The nickel–amidophosphine complexes $[\{\text{Bu}^t\text{OP}(\mu\text{-NBu}^t)_2\text{PNBu}^t\}\text{NiCl}(\text{PBU}^n_3)]$, $[(\text{PBU}^n_3)\text{ClNi}\{\text{Bu}^t\text{NP}(\mu\text{-NBu}^t)_2\text{PNBu}^t\}\text{NiCl}(\text{PBU}^n_3)]$, and $[\{\text{Me}_2\text{Si}(\mu\text{-NBu}^t)_2\text{PNBu}^t\}\text{NiCl}(\text{PBU}^n_3)]$ were synthesized and X-ray structurally characterized. In these mono- and di-nuclear nickel complexes the nickel ions are coordinated in pseudo square-planar fashions, by one trialkylphosphine ligand, one chloride ligand and one $\kappa P, N$ -coordinated amidophosphine moiety from *tert*-butylamido-substituted heterocycles. Attempts to create nickel complexes chelated in a $\kappa^2 P$ fashion by the *o*-phenylenediamine-tethered mono- and di-anionic 1- $\{\text{Me}_2\text{Si}(\mu\text{-NBu}^t)_2\text{PN}\}$ 2- $\{\text{Me}_2\text{Si}(\mu\text{-NBu}^t)_2\text{PNH}\}\text{C}_6\text{H}_4$ and 1,2- $\{\text{Me}_2\text{Si}(\mu\text{-NBu}^t)_2\text{PN}\}\text{C}_6\text{H}_4$, respectively, afforded instead $[1,2\text{-}\{\text{Me}_2\text{Si}(\mu\text{-NBu}^t)_2\text{PN}\}\{\text{Me}_2\text{Si}(\mu\text{-NBu}^t)_2\text{PN}\}\text{C}_6\text{H}_4\text{NiCl}]$ and $[1,2\text{-}\{\text{Me}_2\text{Si}(\mu\text{-NBu}^t)_2\text{PN}\}\text{-}\{\text{Me}_2\text{Si}(\mu\text{-NBu}^t)_2\text{PN}\}\text{C}_6\text{H}_4\text{Ni}\{\text{PEt}_3\}]$, each complex having $\kappa P, N$ and κP coordinated amidophosphine ligands.

Introduction

The Group 15 elements nitrogen and phosphorus form compounds of an unusual structural variety and exhibit more bonding modes than any other pair of congeners in the periodic table.¹ Among the most common phosphorus–nitrogen compounds are tris(amino)phosphines, *e.g.*, $\text{P}(\text{NR}_2)_3$, the isoelectronic analogs of tertiary phosphines. As neutral molecules, these ambidentate ligands, with their adjacent hard- and soft-donor elements, coordinate transition metals almost exclusively *via* their phosphorus atoms. Their structural, and even their electronic, properties thus mirror those of tertiary phosphines in most respects.

Aminophosphines bearing at least one primary amine can be deprotonated to furnish amidophosphines.² Although such anions are usually depicted with the negative charge localized on the nitrogen atom, this is not only an oversimplification, but often an incorrect representation of the true nature of these species. Supporting evidence has come from both the reaction- and the coordination-chemistry of these anions. Thus, amidophosphines react with electrophiles *via* nitrogen or phosphorus,³ depending upon the electrophile and the reaction conditions. The ambidentate amidophosphines have been shown to chelate metals through either nitrogen (κN),⁴ phosphorus (κP)⁵ or through both atoms simultaneously ($\kappa P, N$).^{6–8}

Depending on one's inclination the bis(*tert*-butylamino)-diazadiphosphetidine **1** (Chart 1) may be regarded as either a cyclic diphosphine or a cyclic tetraamine.⁹ In the former role this heterocycle had garnered some attention as neutral phosphorus-donor ligand for transition metals.^{10–12} A number of nickel complexes of such neutral diazadiphosphetidines had also been claimed, but to our knowledge, none of these was fully characterized nor had a crystal structure determination appeared. We were particularly intrigued by reports in which the

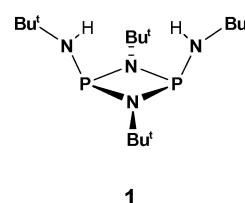


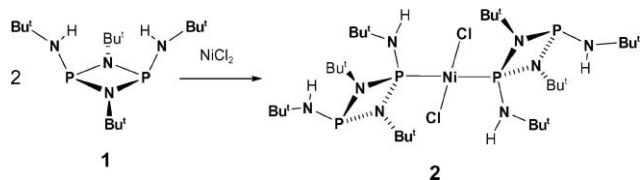
Chart 1

coordination of both phosphorus atoms of one diazadiphosphetidine ring to one nickel center was proposed,¹³ because the nearly planar structure of the P_2N_3 heterocycle made this seem impossible. As a neutral tetraamine ligand, **1** may be expected to chelate metal atoms through two or more of its nitrogen atoms, but we are unaware of any example of a metal coordinated by a neutral diazadiphosphetidine solely through nitrogen.

In the following we describe nickel complexes in which amino- and amido-phosphines coordinate metals through either phosphorus alone or through phosphorus and nitrogen simultaneously. We also attempt to shed some light on the chameleonic behavior of the anionic amidophosphines as ligands in coordination chemistry and offer suggestions on how these ambidentate ligands may be tuned to favor one coordination mode over another.

Results

The interaction of nickel(II) chloride with two equivalents of *cis*- $\{\text{Bu}^t(\text{H})\text{NP}(\mu\text{-NBu}^t)_2\text{PN}(\text{H})\text{Bu}^t\}$ in refluxing toluene (Scheme 1) furnished dark-red **2**, which crystallized with one molecule of toluene per complex. Both the ¹H and ³¹P NMR spectra immediately showed that the diazadiphosphetidine



Scheme 1

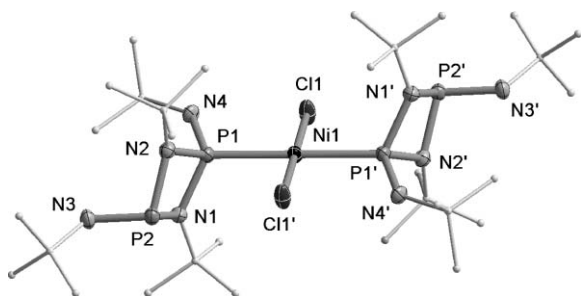


Fig. 1 Thermal ellipsoid (30%) plot and partial labeling scheme of **2**. The solvent molecule (toluene) and the hydrogen atoms have been omitted and the *tert*-butyl groups are drawn as sticks. The atoms with primed labels are related to those with plain labels by the symmetry operation $1 - x, 1 - y, -z$. Selected bond lengths (Å) and angles (°): Ni1–Cl1 2.1661(13), Ni1–P1 2.2763(13), P1–N4 1.644(3), P2–N3 1.669(4); Cl1–Ni1–P1 86.45(5), Cl1–Ni1–P1' 93.55(5).

ligands were coordinated through one phosphorus atom only. Thus there were two signals, at 71.8 and 30.1 ppm, respectively, in the ^{31}P NMR spectrum, indicative of free and coordinated phosphorus atoms, as well as two sets of signals for the tertiary butyl groups and the two amino hydrogen atoms of the ligands. A single-crystal X-ray analysis of **2** (Fig. 1) showed that the diazadiphosphetidine ligands were indeed not chelating, but that they served as monodentate aminophosphines instead. The crystal data and refinement parameters are listed in Table 1.

Complex **2** is located on a crystallographic inversion center and thus has *trans* geometry. The nickel atom lies on the inversion center and heterocycles are orthogonal to the coordination plane, placing the *tert*-butylamino groups in the plane of the metal and the endocyclic nitrogen atoms and their *tert*-butyl substituents perpendicular to it. The *tert*-butylamino groups attached to the coordinated phosphorus atom have an endo conformation, while those on the free phosphorus atom are exo. Due to inductive effects exerted by the metal atom, the endocyclic and exocyclic P–N bonds are contracted to 1.644(3) and 1.694(4) Å, respectively, from 1.664(2) and 1.725(2) Å in **1**.¹⁴ The sum of the N–P–N bond angles of the coordinated phos-

phorus atom ($\sum_{\text{N-P-N}}$) is 310.3°, making this phosphorus atom significantly less pyramidal than the uncoordinated phosphorus atom (289°). This flattening of the phosphorus atoms is due to the conversion of the lone pair of electrons to a bond pair and, as will be seen below, it increases with increasing metal–phosphorus interaction. The isolation of **2** is further evidence that neutral bis(1°-amino)diazadiphosphetidines act as phosphorus, rather than nitrogen, donors towards late transition metals, and that they coordinate these in a monodentate fashion.

To compare the bond parameters of **2** with those of a bis(trialkylphosphine)nickel dichloride complex, we synthesized *trans*-[NiCl₂(PEt₃)₂] (**3**) according to a published procedure and conducted a single-crystal X-ray analysis of the cherry-red crystals.¹⁵ Crystal and refinement data are summarized in Table 1, while Fig. 2 is a perspective view of this classic nickel complex. The partially-refined structure of the bromide analogue, *trans*-[NiBr₂(PEt₃)₂], had appeared previously,¹⁶ but to our knowledge a single-crystal X-ray analysis of **3** has not been reported. These bromide and chloride complexes are isomorphous, but we chose a different unit cell for the refinement of **3**. In *trans*-[NiBr₂(PEt₃)₂] the nickel–bromide (2.26 Å) and nickel–triethylphosphine (2.30 Å) bonds, enclose angles of almost exactly 90°.

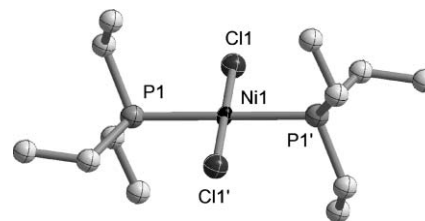


Fig. 2 Thermal ellipsoid (30%) plot and partial labeling scheme of **3**. Hydrogen atoms have been omitted. Selected bond lengths (Å) and angles (°): Ni1–Cl1 2.1628(5), Ni1–P1 2.2329(5); Cl1–Ni1–P1 87.29(2), Cl1–Ni1–P1' 92.71(2). The atoms with primed labels are related to those with plain labels by the symmetry operation $-x, 2 - y, -z$.

It is fortuitous that both **2** and **3** are *trans* isomers, because this makes the comparison of their structural parameters more meaningful. Although the diazadiphosphetidine is much bulkier than triethylphosphine, the structural similarities of both complexes are immediately apparent. Just as in **2**, the nickel ion, the chloride ligands and the phosphorus atoms of **3**, together with their central ethyl substituents, all lie in the coordination plane. The Cl–Ni–Cl and P–Ni–P bonds angles in both complexes are rigorously 180°, but the Cl–Ni–P bond angles deviate slightly from 90°, the acute angles being 86.45(5)° in **2** and 87.29(2)°

Table 1 Crystal and refinement data for **2**, **3** and **8**

Compound	2	3	8
Formula	C ₃₉ H ₇₆ Cl ₂ N ₈ NiP ₄	C ₁₂ H ₃₀ Cl ₂ NiP ₂	C ₂₆ H ₆₀ ClN ₃ NiP ₂ Si
Formula weight	910.57	365.91	598.96
Crystal system	Monoclinic	Monoclinic	Monoclinic
Space group	<i>P</i> 2 ₁ / <i>n</i> (no. 14)	<i>P</i> 2 ₁ / <i>n</i> (no. 14)	<i>P</i> 2 ₁ / <i>c</i> (no. 14)
<i>a</i> /Å	9.541(2)	7.3453(10)	10.8581(13)
<i>b</i> /Å	10.730(2)	11.4847(15)	21.494(3)
<i>c</i> /Å	25.185(6)	10.8061(14)	15.1459(17)
β /°	95.92(2)	90.990(2)	93.934(2)
<i>U</i> /Å ³	2564.7(10)	911.5(2)	3526.6(7)
<i>Z</i>	2	2	4
μ /mm ⁻¹	0.641	1.515	0.768
Reflections collected	12945	5935	25345
Independent reflections (<i>R</i> _{int})	4389 (0.0671)	3311 (0.0336)	8743 (0.0467)
<i>R</i> (<i>F</i>), ^a (<i>I</i> > 2 σ <i>I</i>)	0.0561	0.0291	0.0517
<i>wR</i> 2(<i>F</i> ²), ^b all data	0.1450	0.1058	0.1660
ρ /e Å ⁻³	1.192, –0.384	0.355, –0.225	0.840, –0.444

^a $R = \sum |F_o - F_c| / \sum |F_o|$. ^b $wR2 = \{[\sum w(F_o^2 - F_c^2)^2] / [\sum w(F_o^2)^2]\}^{1/2}$; $w = 1 / [\sum^2(F_o^2) + (xP)^2 + yP]$ where $P = (F_o^2 + 2F_c^2) / 3$.

in **3**. The nickel–chloride bond lengths in **2** (2.1662(13) Å) and **3** (2.1628(5) Å) are equal within experimental errors, but the Ni–P bond to the heterocyclic phosphine is somewhat longer (2.2763(13) Å) than that to triethylphosphine (2.2329(5) Å). Despite this slight discrepancy, the almost identical bond parameters about nickel in these two square-planar complexes are nonetheless remarkable. Our data thus seem to confirm that, at least when coordinated to nickel(II) ions, aminophosphines and trialkylphosphines have similar ligating properties.

A significant difference between aminophosphines and trialkylphosphines is that the former can be readily converted to anionic ligands, provided that at least one primary amino group is present. We, therefore, chose to investigate the coordination chemistry of nickel with anionic bis(1°-amido)diazadiphosphetidines, which had proven to be a fertile ground for unusual coordination modes and molecular structures in both main group and transition metal chemistry.^{17–20} Deprotonation of the bis(*tert*-butylamino)diazadiphosphetidine **1** with strong bases (e.g., BuⁿLi) and subsequent treatment with metal halides had furnished the corresponding metal derivatives. Most of these adopted one of two structure types, namely **A** or **B** (Chart 2), demonstrating that anionic bis(*tert*-butylamido)diazadiphosphetidines show a strong preference to coordinate metals through nitrogen.

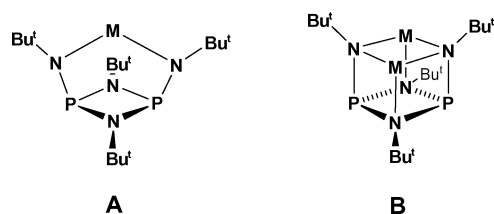
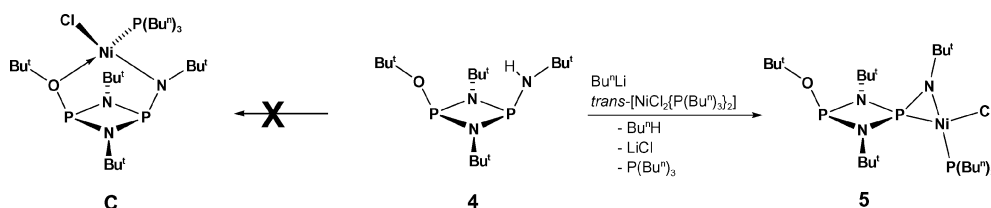


Chart 2

For applications in catalysis we attempted to synthesize a mono-amido diazadiphosphetidine with an oxygen-donor functionality (Scheme 2). To this end we modified **1** by replacing one *tert*-butylamino group with a *tert*-butoxy group to obtain the asymmetric diazadiphosphetidine (**4**). Deprotonation of **4** with BuⁿLi and subsequent treatment with *trans*-[NiCl₂(P(Buⁿ)₃)₂] (Scheme 2), however, did not afford the expected *N,O*-chelated nickel complex **C**. Instead, we isolated a dark-red crystalline compound that was shown by NMR spectroscopy and X-ray techniques to be the nickelaazaphosphirane **5**; that is, a complex in which the ligand coordinated the metal laterally in a $\kappa P,N$ fashion. Apparently the late transition metal nickel preferred the formation of a three-membered Ni–P–N ring over the more conventional chelation by oxygen and nitrogen above the heterocycle. The solid-state structure of **5** is shown in Fig. 3; selected bond parameters are collected in Table 2.

Complex **5** has crystallographic *m* symmetry and thus features a rigorously planar nickel(II) coordination environment, which is composed of the amidophosphine moiety of a *cis*-configured P(*tert*-butoxy)-P(*tert*-butylamido)diazadiphosphetidine, one tri(*n*-butyl)phosphine molecule and one chloride ligand. The tertiary butyl group attached to the oxygen atom is *exo* with respect to the P₂N₂ heterocycle, while that on N1 has an *endo* conformation. This nickel complex does not



Scheme 2

Table 2 Selected bond lengths (Å) and angles (°) for **5**, **6** and **8**

	5	6	8
Ni–Cl	2.2175(10)	2.1998(16) av.	2.2209(7)
Ni–N	1.925(3)	1.942(4) av.	1.939(2)
Ni–P(ring)	2.0796(9)	2.0749(14) av.	2.0693(7)
Ni–PR ₃	2.1522(12)	2.1567(17) av.	2.1399(8)
P–N(exo)	1.559(3)	1.554(4) av.	1.560(2)
P–N(endo) av.	1.699(2)	1.692(4)	1.680(2)
Si–N av.	n.a.	n.a.	1.747(2)
P–Ni–Cl	151.17(4)	150.71(6) av.	153.06(3)
PR ₃ –Ni–Cl	92.95(5)	95.44(7) av.	96.86(3)
N–Ni–Cl	105.55(9)	105.50(13) av.	107.42(6)
P–Ni–PR ₃	115.88(5)	113.84(6) av.	110.08(3)
N–Ni–P	45.62(9)	45.36(12) av.	45.66(6)
Ni–P–N	61.93(11)	62.78(15) av.	62.74(8)
Ni–N–P	72.45(12)	71.87(15) av.	71.60(9)

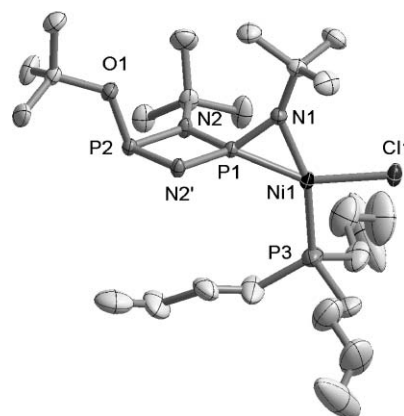
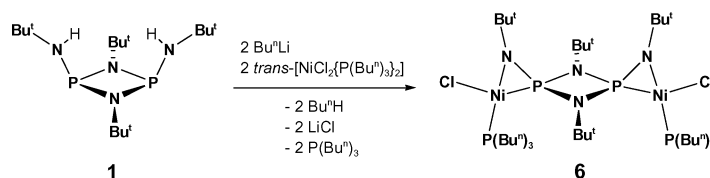


Fig. 3 Thermal ellipsoid (30%) plot and partial labeling scheme of **5**. The hydrogen atoms and the *tert*-butyl group on N2' have been omitted to enhance clarity. N2' was generated from N2 by the symmetry operation $x, -y + 0.5, z$.

adopt a standard coordination geometry, but the structure is closest to square planar. Due to the very acute endocyclic nickelaazaphosphirane angle 45.62(9)° at nickel only the Cl1–Ni1–P3 angle (92.95(5)°) has a value that is close to ideal square-planar geometry. The N1–Ni1–Cl1 (105.55(9)°) and P1–Ni1–P3 (115.88(5)°) angles, in turn, are intermediate between square planar and trigonal planar. The nickel–P3 (2.1522(12) Å) and the nickel–chloride (2.2175(10) Å) bonds have normal lengths, but the bond to N1 (1.925(3) Å) is slightly elongated. The nickel bond to the phosphorus atom of the heterocycle (P1), by contrast, is only 2.0796(9) Å long, and the coordinated phosphorus–nitrogen bond (P1–N1) has undergone an even greater contraction to 1.559(3) Å, indicative of a change to double-bond order. Here \sum_{N-P-N} at P1 has increased to 334.0°, which is another reflection of the much stronger metal–ligand interaction in this complex vs. that in **2**.

Three-membered rings are highly strained, and there is a bias against proposing such structures even though in transition metal chemistry three-membered rings are not uncommon. Nickel, in particular, seems to have a propensity to form three-membered metalacycles as exemplified by numerous



Scheme 3

metalacyclopropanes,²¹ metalacyclopropenes²² and three-membered nickelacycles involving main group atoms other than carbon.²³ The isolation and stability of **5** further supported this notion, because the *P*-amidodiazadiphosphetidine complexes of nickel form exceptionally strong and symmetrical M–P and M–N bonds,²⁴ and we therefore decided to study these systems in more detail. The obvious starting point for this investigation was the di(*tert*-butylamino)diazadiphosphetidine **1**, which in its dianionic form had produced only bis(amido) complexes of structure types **A** or **B**. The dianion of **1** reacted with two equivalents of *trans*-[NiCl₂(P(Buⁿ)₃)₂], as shown in Scheme 3, to furnish the bis(nickelazaphosphirane) **6**. Because no metal had previously been coordinated by this ligand in this manner, the reaction confirmed that nickel has an inherent preference to coordinate amidophosphines based on heterocyclic scaffolds in a κ*P,N* fashion. The solid-state structure of **6** is shown in Fig. 4; selected bond parameters are given in Table 2.

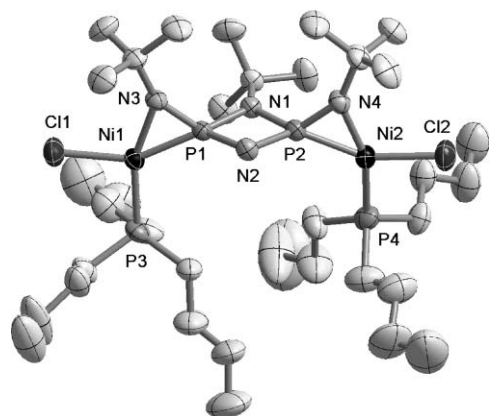
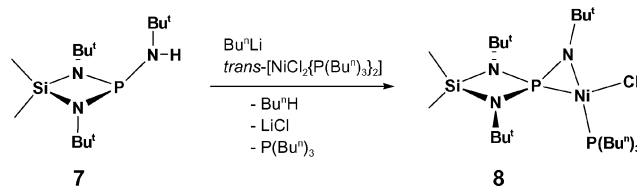


Fig. 4 Thermal ellipsoid (30%) plot and partial labeling scheme of **6**. The hydrogen atoms and the *tert*-butyl group attached to N2 have been omitted.

The dispirocyclic complex has non-crystallographic *C*₂ symmetry and features two nickelazaphosphirane rings which cap the diazadiphosphetidine laterally. Overall, the structure is dominated by the two bulky *C*₃-symmetric tri(*n*-butyl)phosphine ligands. For steric reasons both *tert*-butyl groups of the amido nitrogen atoms (N3 and N4) have endo conformations, that is, they are tipped towards the P₂N₂ heterocycle. The bond parameters of the nickel ions are isometric and almost identical to those of the nickel ion in **5**. Only the nickel–chloride bonds, which average 2.1998(16) Å, are somewhat shorter than in the mono-nickel complex.

Syntheses and structures of **5** and **6** were previously communicated.²⁵ The difunctional ligands in these complexes can create both structural and analytical problems and to simplify the coordination chemistry of these heterocycles we replaced one of the PN(H)Bu^t groups of **1** with a Me₂Si group to obtain the diazaphosphasiletidine {Me₂Si(μ-NBu^t)₂PN(H)Bu^t} (**7**).²⁶ This silicon-phosphorus–nitrogen compound retains the essential structure of the phosphorus–nitrogen ligands, namely a phosphorus(III) atom incorporated in a heterocycle and flanked by two sp²-hybridized nitrogen atoms. Deprotonation of **7** and subsequent treatment of the anion with *trans*-[NiCl₂(P(Buⁿ)₃)₂] (Scheme 4) produced the red, diamagnetic nickel complex **8**, whose NMR spectra identified it as a structural analogue of **5** and **6**.



Scheme 4

Crystal and refinement data for **8** are collected in Table 1 and selected bond parameters are listed in Table 3. With the exception of the dimethylsilyl group which now caps one corner of the heterocycle, the solid-state structure of **8** (Fig. 5) mirrors that of **5**. All bonds to nickel are almost identical to those in **5** and **6**, indicating that the inclusion of silicon into the heterocycle has had no effect on the bonding parameters of the nickelazaphosphirane moiety.

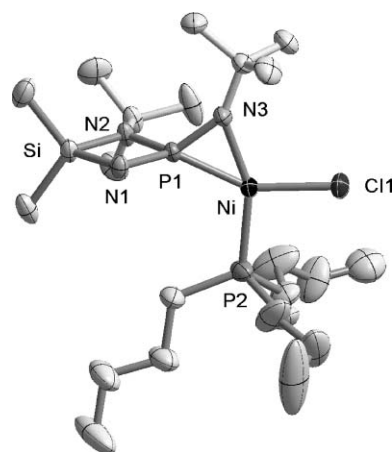


Fig. 5 Thermal-ellipsoid (30%) plot and partial labeling scheme of **8**. Hydrogen atoms and the tertiary butyl group on N1 have been omitted.

The metalacyclic structures of **5**, **6** and **8** are reflected in their ³¹P NMR spectra. Thus, for example, the signals for the phosphorus atoms incorporated in these three-membered rings appear at –53.6, –82.4 and –53.9 ppm, respectively, while those for the free ligands *cis*-{Bu^t(H)NP(μ-NBu^t)₂POBu^t}, *cis*-{Bu^t(H)NP(μ-NBu^t)₂PN(H)Bu^t} and {Me₂Si(μ-NBu^t)₂PN(H)Bu^t} appear at 103.9, 88.5 and 114.8 ppm, respectively. These coordination upfield shifts of about 157–170 ppm far exceed those of neutral diazadiphosphetidines or trialkylphosphines, which typically move *ca.* 50 ppm to higher field or *ca.* 40 ppm to lower field, upon metal coordination.

These findings on **5**, **6** and **8** confirmed that heterocyclic amidophosphines have a strong preference to coordinate nickel through both phosphorus and nitrogen. To test just how strong the preference for this coordination mode was, we deliberately tried to prevent it. We anticipated that a bis(amidodiazaphosphasiletidine), connected by a suitable organic linker, would introduce sufficient bond strain in a κ²*P*,κ²*N* bonding mode (**D**, Chart 3) to make such a chelation all but impossible. It appeared more likely that a dianionic ligand would prefer to bind nickel in a less strained κ²*P* fashion (**E**). For the synthesis of such a chelating ligand we treated dilithium *o*-phenylenediamide with two equivalents of the *P*-chlorodiazaphosphasiletidine (Scheme 5). Similar

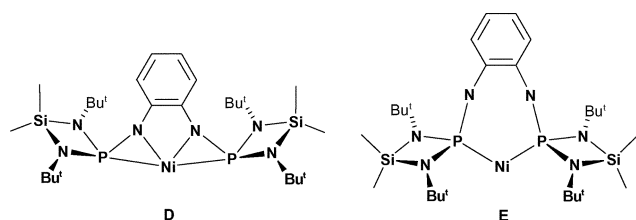
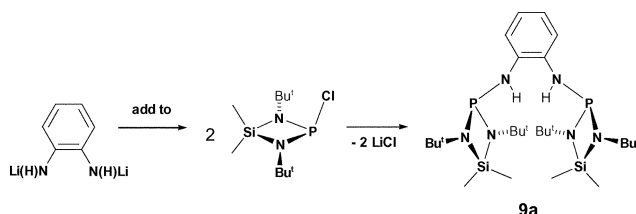


Chart 3



Scheme 5

o-phenylenediamine-based bis(aminophosphines), bearing diphenylphosphino moieties, are well known.²⁷

Although this ligand synthesis seemed straightforward, the manner in which the dianion and the chlorophosphine were combined was crucial for the outcome of the reaction. Thus, the addition of 1,2-(Li(H)N)₂C₆H₄ to Me₂Si(μ-NBu')₂PCl (Scheme 5) afforded only the targeted symmetrical disubstitution-product **9a** in 86% yield, while the reverse order of addition (Scheme 6) produced a mixture of symmetrical (**9a**) and asymmetrical disubstitution (**9b**) products in an overall yield of 69%. This latter compound, an *N,N*-diphosphinoamine, has applications in its own right and although both isomers can be cleanly separated by fractional crystallization, the former route is obviously preferable for the ligand synthesis.

The formation of the asymmetric product **9b** in Scheme 6, can be rationalized in terms of the intermolecular 1,4-proton shift shown in Scheme 7. When the chlorophosphine is added

to the dilithio-*ortho*-phenylenediamine, the dianion is in excess until the reaction is completed and a high concentration of the monosubstituted, monoanion **9** is present at all times. This monoanion has sufficient time to undergo a 1,4-proton shift to furnish an amidophosphine and an NH₂ group before it is trapped by the second equivalent of chlorophosphine, producing **9b**. This mechanism implies that the PNH moiety is more acidic than the NH₂ moiety, and given the charge delocalization in the anionic PN group discussed below, this is not an unreasonable suggestion. If the dianion is added to a solution of Me₂Si(μ-NBu')₂PCl (Scheme 5), the dianion is trapped by two equivalents of the chlorophosphine, before the proton transfer can occur, and only the symmetric product **9a** is formed.

Single-crystal X-ray analyses of **9a** and **9b** revealed the expected structures. Crystal and refinement data are listed in Table 3, while selected bond parameters for **9a** are given in Table 4. Fig. 6 shows a perspective view of **9a** that emphasizes the perpendicular orientation of the almost parallel inorganic heterocycles with respect to the aromatic ring. The conformations about the exocyclic P–N bonds are *exo*, *i.e.*, the lone-pairs of electrons on the phosphorus atoms are pointing outward

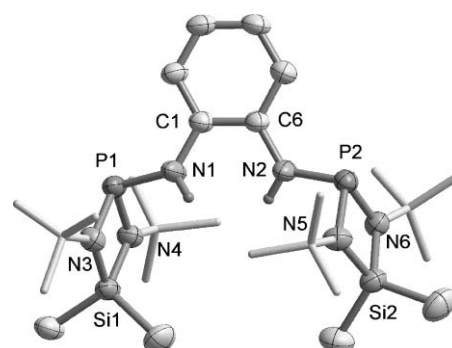
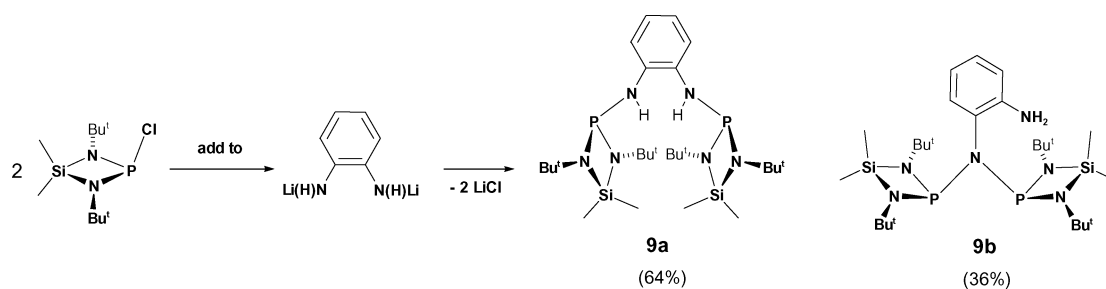
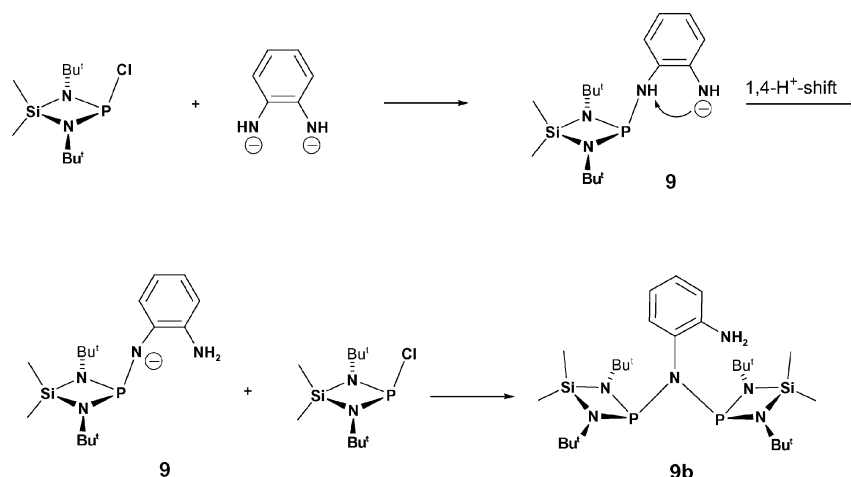


Fig. 6 Thermal ellipsoid (30%) plot and partial labeling scheme of **9a**. All but the amino hydrogen atoms have been omitted, and the *tert*-butyl groups are drawn as sticks only.



Scheme 6



Scheme 7

Table 3 Crystal and refinement data for **9a–11**

Compound	9a	9b	10	11
Formula	C ₂₆ H ₅₄ N ₆ P ₂ Si ₂	C ₂₆ H ₅₄ N ₆ P ₂ Si ₂	C ₃₃ H ₆₁ ClN ₆ NiP ₂ Si ₂	C ₃₂ H ₆₇ N ₆ NiP ₃ Si ₂
Formula weight	568.87	568.87	754.16	743.72
Crystal system	Monoclinic	Orthorhombic	Monoclinic	Triclinic
Space group	<i>P</i> 2 ₁ / <i>c</i> (no. 14)	<i>Pbca</i> (no. 61)	<i>P</i> 2 ₁ / <i>n</i> (no. 14)	<i>P</i> $\bar{1}$ (no. 2)
<i>a</i> /Å	9.2122(13)	12.225(3)	10.6331(13)	11.4153(15)
<i>b</i> /Å	33.045(5)	16.738(4)	15.7716(15)	12.2457(16)
<i>c</i> /Å	12.3486(16)	32.714(7)	25.212(2)	16.145(2)
<i>a</i> /°				79.259(2)
<i>β</i> /°	109.808(10)		93.343(8)	79.351(2)
<i>γ</i> /°				69.353(2)
<i>U</i> /Å ³	3536.7(8)	6712(2)	4220.8(8)	2057.4(5)
<i>Z</i>	4	8	4	2
<i>μ</i> /mm ⁻¹	0.214	0.228	0.685	0.675
Reflections collected	5826	5433	7138	10494
Independent reflections (<i>R</i> _{int})	4593 (0.0221)	4355 (0.0468)	5506 (0.0238)	7116 (0.0556)
<i>R</i> (<i>F</i>) ^a (<i>I</i> > 2σ <i>I</i>)	0.0588	0.0548	0.0520	0.0505
<i>wR</i> 2(<i>F</i> ²) ^b all data	0.1772	0.1536	0.1444	0.1297
<i>ρ</i> /e Å ⁻³	0.455, -0.299	0.357, -0.402	0.586, -0.372	0.987, -0.407

^a *R* = $\sum |F_o - F_c| / \sum |F_o|$. ^b *wR*2 = $\{[\sum w(F_o^2 - F_c)^2] / [\sum w(F_o^2)^2]\}^{1/2}$; *w* = $1 / [\sum^2(F_o)^2 + (xP)^2 + yP]$ where *P* = $(F_o^2 + 2F_c^2) / 3$.

Table 4 Selected bond lengths (Å) and angles (°) for **9a**, **10** and **11**

	9a	10	11
Ni1–Cl1/P3		2.1640(13)	2.1383(11)
Ni–N1		1.835(3)	1.856(3)
Ni–P1		2.1783(12)	2.1603(11)
Ni–P2		2.1456(11)	2.1756(11)
P1–N1	1.704(3)	1.603(4)	1.592(3)
P2–N2	1.694(3)	1.668(3)	1.605(3)
P1–N(endo) av.	1.712(3)	1.682(3)	1.684(3)
P2–N(endo) av.	1.712(3)	1.679(3)	1.714(3)
Si1–N(endo) av.	1.715(3)	1.738(3)	1.730(3)
Si2–N(endo) av.	1.716(3)	1.733(3)	1.729(3)
N1–C1	1.405(4)	1.389(6)	1.398(4)
N2–C6	1.404(4)	1.400(5)	1.360(5)
C1–C6	1.391(5)	1.393(6)	1.432(5)
P1–Ni1–Cl1/P3		119.20(5)	117.01(4)
P1–Ni1–N1		46.10(11)	45.93(9)
N1–Ni1–P2		95.46(11)	92.57(10)
P2–Ni1–Cl1/P3		99.24(5)	104.48(4)
Ni1–N1–P1		78.30(15)	77.16(13)
Ni1–P1–N1		55.60(12)	56.91(11)
Ni1–P2–N2		108.52(12)	112.53(12)

and away from each other. A similar structure was recently reported for a macrocycle composed of two diazadiphosphetidine molecules connected by two *o*-phenylenediamine linkers, where geometric constraints dictate an *exo* conformation.²⁸ The six crystallographically unique phosphorus–nitrogen bonds of **9a** are almost isometric, ranging from 1.694(3) to 1.715(3) Å, while the silicon–nitrogen bonds are rigorously isometric (1.715(3) Å).

In **9b** (Fig. 7) the diazaphosphasetidine rings are both attached to the same nitrogen atom of the *o*-phenylenediamine, making it a diposphinoamine. The molecule exhibits a rotational disorder in the solid state, with the NH₂ group of the aromatic diamine occupying two positions, which are related to each other by a non-crystallographic C₂ axis coinciding with the N5–C50 bond. The greater steric crowding in **9b** is reflected in elongated phosphorus–nitrogen (1.740(3) Å) and silicon–nitrogen (1.735(3) Å) bonds compared to those in **9a**.

For the synthesis of the targeted nickel complex, we treated **9a** with two equivalents of *n*-butyllithium, and added the ensuing dilithium derivative to a suspension of anhydrous nickel(II) chloride, as outlined in Scheme 8. The ³¹P NMR spectrum of the maroon product, however, showed an AB pattern of doublets at 94.7 and –28.3 ppm, respectively, which was inconsistent with a symmetrical structure. The doublet at –28.3 ppm suggested

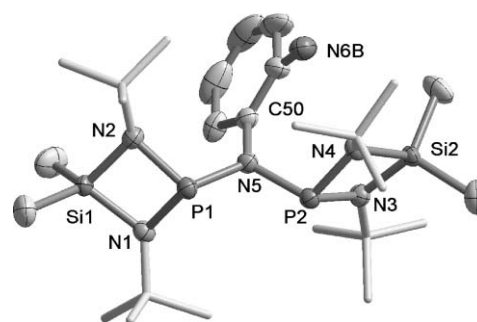
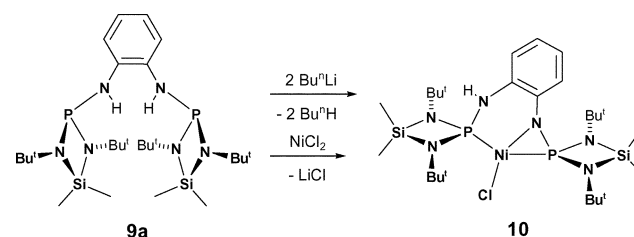


Fig. 7 Thermal ellipsoid (30%) plot and partial labeling scheme of **9b**. Only one of the two locations of the amino nitrogen atom (6B) is shown. All hydrogen atoms have been omitted and the *tert*-butyl groups are drawn as sticks only. Selected bond lengths (Å) and angles (°): P1–N5 1.758(3), P2–N5 1.752(3), P1–N(endo) av. 1.730(3), P2–N(endo) av. 1.729(3), P1–N5–P2 108.97(15).

**Scheme 8**

the presence of a nickelazaphosphirane, while the low field signal was typical of diazadiphosphetidines coordinated through phosphorus only. Both doublets were shifted to high field by about 25 and 148 ppm, respectively, the latter shift difference being quite similar to those for the metalacyclic phosphorus atoms in **5**, **6** and **8**. Even more intriguing than the chemical-shift differences of the two signals was the unusually large phosphorus–phosphorus coupling constant of 667 Hz, which is as large, or larger, than those in compounds with direct phosphorus–phosphorus bonds.¹

To obtain conclusive structural information on **10** we analyzed it by single-crystal X-ray methods. A thermal ellipsoid plot of the solid-state structure of **10** is shown in Fig. 8. Crystal and refinement data are collected in Table 3, while selected bond parameters are listed in Table 4. The presence of the chloride ligand in **10** immediately indicated that the chelating bis(diazaphosphasetidine) ligand was only monoanionic. Our

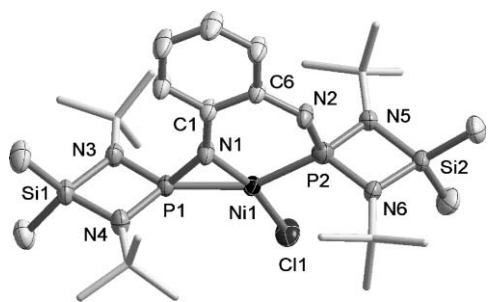


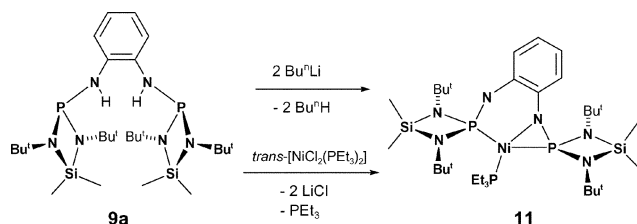
Fig. 8 Thermal ellipsoid (30%) plot and partial labeling scheme of **10**. All hydrogen atoms have been omitted and the *tert*-butyl groups are drawn as sticks only.

failure to obtain the dianion may have been the result of the incomplete deprotonation of the chelating ligand or the presence of adventitious water in the nickel(II) chloride, but the latter scenario is more likely. While the complex is structurally more elaborate than **5**, **6** and **8**, the coordination environment about nickel is rather similar. It is convenient to consider **10** a nickelaazaphosphirane in which the nickel ion is coordinated by an amido nitrogen atom (N1), bearing an aromatic, rather than a *tert*-butyl, substituent. Tethered to the *ortho* position of this aromatic ring is a second aminodiazaphosphasiletidine which binds the nickel center as a neutral, heterocyclic phosphine.

Due to the chelating nature of **9a**, the amido nitrogen (N1) is now *trans* ($165.29(12)^\circ$) to the chloride ligand, while the two phosphorus atoms have pseudo-*trans* ($141.56(5)^\circ$) geometry. The nickel atom and the ligand donor atoms are again in a planar coordination environment, but there is significant folding of the molecule along the N1–N2 vector. Thus, the plane defined by nickel and its nearest atomic neighbors (N1, P1, P2, Cl1) and that defined by N1, N2, C1 and C6 enclose an angle of *ca.* 14° . The Ni1–P1 ($2.1783(12)$ Å) and Ni1–P2 ($1.603(4)$ Å) bonds are somewhat longer than those in **5**, **6** and **8**, but the Ni1–N1 bond is *ca.* 0.1 Å shorter ($1.835(3)$ Å). The nickel–chloride bond ($2.1640(13)$ Å) is also shorter than those in **5**, **6** and **8**. These bond differences are likely at least partially due to different atoms being in a *trans* configuration to each other.

For electron-counting purposes, and using a covalent bonding model, the P–N moiety is a three-electron donor, while P2 and Cl1 are two- and one-electron donors, respectively. This makes **10** a 16-electron species—a reasonable electron count for a diamagnetic, pseudo-square planar nickel complex.

To synthesize a chloride-free nickel complex of **9a**, we repeated the reaction (Scheme 9), but with *trans*-[NiCl₂(PEt₃)₂] as a soluble and more reliable source of anhydrous nickel(II). This reaction produced a visibly different, almost black, solution. The ³¹P NMR spectrum of the product exhibited three signals, namely two doublets of doublets at 78.1 and -6.3 ppm, respectively, but with a reduced coupling constant of 413 Hz. An unresolved multiplet at 20.5 ppm for coordinated triethylphosphine suggested the absence of the chloride ligand.



Scheme 9

The solid-state structure of **11**, shown in Fig. 9, confirmed this suspicion as it is essentially identical to that of **10**, but with a triethylphosphine moiety in place of the chloride ion. Crystal and data collection parameters are provided in Table 2,

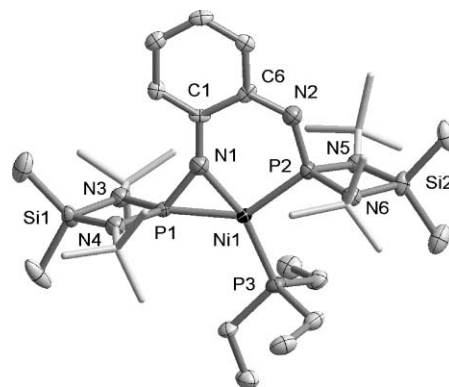


Fig. 9 Thermal ellipsoid (30%) plot and partial labeling scheme of **11**. All hydrogen atoms have been omitted and the *tert*-butyl groups are drawn as sticks only.

while selected bond parameters are juxtaposed to those of the corresponding bonds for **9a** and **10** in Table 4. Although here the chelating ligand is dianionic, only one amidophosphine moiety is coordinated in a $\kappa P,N$ fashion, while the second one is bound through phosphorus only. This raises the question whether the negative charge is localized on N2 or delocalized. The notion that the additional negative charge is substantially delocalized over the entire molecule is supported by the perfect planarity of the plane defined by almost all the heavy atoms. Only the nitrogen atoms of the diazaphosphasiletidines (N3 through N6), their *tert*-butyl substituents and the two lateral ethyl groups of the triethylphosphine ligand do not lie in this plane. The presumed charge delocalization in **11** is further revealed by the bond parameters involving nitrogen atom N2. For example, the P2–N2 ($1.605(3)$ Å) and N2–C6 ($1.360(5)$ Å) bonds are significantly shorter than those in **10**, while the aromatic bond from C1 to C6 has lengthened from $1.392(4)$ to $1.432(5)$ Å. Also elongated are the nickel–P2 bond ($2.1756(11)$ Å) and the endocyclic P2–N5 and P2–N6 bonds, which now average $1.714(4)$ Å. The nickel bond to triethylphosphine ($2.1383(11)$ Å), by contrast, has the same length as the nickel bond to the tri(*n*-butyl)phosphine ligand in **8**.

Despite the almost identical structures of **10** and **11**, the covalent bonding model yields an electron count of seventeen for the nickel center in **11**. From the NMR data it is clear, however, that this is a diamagnetic complex, and this shows that, just like for previously reported anionic phosphine complexes,²⁹ only the ionic bonding model provides a correct electron count. This electron-count discrepancy arises from the fact that a coordinated trivalent phosphorus(III) center, such as P2, is assumed to donate two electrons to the metal in both the ionic- and the neutral-bonding model. Using the ionic model, the nickel(II) center has eight electrons, while the anionic $\kappa P,N$ moiety is assigned four electrons. The anionic κP amidophosphine moiety contributes only two electrons, as does the neutral PEt₃ ligand. This yields a 16-electron count on the nickel center, just as in **10**, where both counting models yield this answer.

Discussion

The neutral bis(*tert*-butylamino)diazadiphosphetidine, **1**, coordinates nickel in a monodentate fashion through phosphorus, rather than nitrogen. Although similar *P*-coordinated diazadiphosphetidine complexes had previously been obtained for somewhat softer rhodium(I)¹⁰ and molybdenum(0) species,¹¹ our results confirm that even divalent nickel prefers a monodentate coordination through phosphorus over a potential chelation by up to four amino nitrogen atoms. Despite its steric bulk **1** forms a square-planar, rather than a tetrahedral, nickel complex with identical stereochemistry and almost identical bond parameters as the much more compact triethylphosphine. These findings

seem to support the commonly held belief that aminophosphines and trialkylphosphines have similar donor/acceptor properties.³⁰

In its anionic form, however, **1** and related amidophosphines based on inorganic-heterocyclic platforms, do not coordinate nickel through nitrogen alone, as they had done in all previously characterized metal complexes of these ligands, but they do so through nitrogen and phosphorus simultaneously. This $\kappa P,N$ coordination creates three-membered rings composed of nickel, phosphorus and nitrogen, so-called nickelaazaphosphiranes. That the thermodynamic driving force for the formation of these three-membered rings is strong is indicated by the absence of any dissociation of the phosphorus atoms in solution and by the unusual shortness of all metalacyclic bonds.

In all three complexes, namely **5**, **6** and **8**, the three-membered metalacycles are almost isometric. Thus, the phosphorus–nitrogen bonds range from 1.554(4) to 1.560(2) Å, the nickel–nitrogen bonds range from 1.925(3) to 1.942(4) Å and the nickel–phosphorus bonds range from 2.0693(7) to 2.0796(9) Å. Importantly, the phosphorus–nitrogen bonds (1.557 Å) are 0.16 Å shorter than the formal single bonds (1.725(2) Å) found in pristine **1** indicating double bond character.¹⁴ The nickel–nitrogen bonds are somewhat longer than for related terminal nickel–organoamido bonds, which range from 1.82 to 1.93 Å.³¹ By contrast, the endocyclic nickel–phosphorus bonds (av. 2.075 Å) are 0.2 Å shorter than the nickel–phosphorus bonds (2.2763(13) Å) to the neutral diazadiphosphetidine in **2**. Despite the apparent angle strain in these rings, the metalacyclic nickel–phosphorus bonds in **5**, **6** and **8** are among the shortest nickel–phosphorus bonds listed in the CCDC Registry for four-coordinate phosphorus(III) species.³²

Although **10** and **11** bear the chelating bis(diazaphosphasetidine) ligand **9a**, which we specifically designed to discourage the $\kappa P,N$ coordination in favor of a κP coordination, both complexes exhibit a mixture of these two bonding modes. Thus, in each complex one nickelaazaphosphirane moiety and one neutral (**10**) or anionic (**11**) heterocyclic phosphine, respectively, are present. The retention of the $\kappa P,N$ coordination in these chelate complexes is further evidence of the favorability of the metalacycle formation. Owing to the fact that the ligand is monoanionic in **10** but dianionic in **11**, the metric parameters of their nickelaazaphosphiranes are not as similar as those in **5**, **6** and **8**. Interestingly, however, the formally anionic phosphine in **11** forms a longer bond with nickel than the neutral phosphine in **10**. Most equivalent bonds of these two latter nickelaazaphosphiranes are almost equidistant, as shown by the phosphorus–nitrogen bonds in **10** (1.603(4) Å) and **11** (1.592(3) Å) and the nickel–nitrogen bonds in **10** (1.835(3) Å) and **11** (1.856(3) Å). It is significant, that the metalacyclic P–N bonds are *ca.* 0.05 Å longer than those in **5**, **6** and **8**, while the Ni–N1 bonds are substantially shorter (*ca.* 0.1 Å). The bond differences of the nickelaazaphosphirane moieties between the two groups (**5**, **6** and **8**) and (**10** and **11**) are due to a number of factors. The latter complexes feature a chelating ligand which imposes certain bond constraints and also places different atoms and groups in *cis/trans* geometries. In **10** and **11** the amidophosphine nitrogen is substituted with an aromatic group, and such electron-withdrawing substituents on the N terminus tend to weaken the phosphorus–nitrogen double bonds of amidophosphines.³³

Metalaazaphosphiranes

Metalaazaphosphiranes had been reported previously, but most were complexes of anilidodiphenylphosphines with a decidedly unsymmetrical bonding pattern between metal and ligand. Thus, in one of the simplest conceivable metalaazaphosphirane, namely the dimeric $[(Et_2O)Li(PhNPPH_2)]_2$ reported by Ashby and Li,² the relevant bond parameters (Li–N 2.023(4) Å, Li–P 3.004(4) Å, P–N 1.672(2) Å) define essentially a metal–

amidophosphine with a weak (but real) Li–P interaction and a phosphorus–nitrogen single bond. The reaction of $Li(PhNPPH_2)$ with zirconium and lanthanide chlorides furnished the eight-coordinate neutral zirconium complex (**G**, Chart 4) and the eight-coordinate anionic lanthanide complexes **H**, respectively. A comparison of the metric parameters in the three-membered rings of **G** and **H** shows that the bonding is also decidedly different from that in the title compounds. That is, the Zr–N (2.175(5) Å) and Zr–P (2.742(2) Å) bonds are comparatively short and long, respectively, while the metalacyclic P–N bond has almost single-bond value, namely 1.666(5) Å.⁴ This asymmetric bond pattern—short M–N bonds but long M–P bonds—is rather similar to that for the lithium derivative and not unexpected for the hard zirconium. The bond asymmetry is also reflected by the solution behavior of the zirconium complex which shows two “free” and two coordinated phosphorus atoms according to ³¹P NMR spectra. An anionic lutetium complex $[(Ph_2PNPh)_4Lu]^-$ (**H**) exhibited an almost identical bond pattern with short Lu–N bonds (2.252(7)–2.272(8) Å) but long Lu–P (2.886(3)–3.040(3) Å) and P–N (1.673(8) Å) bonds.⁸

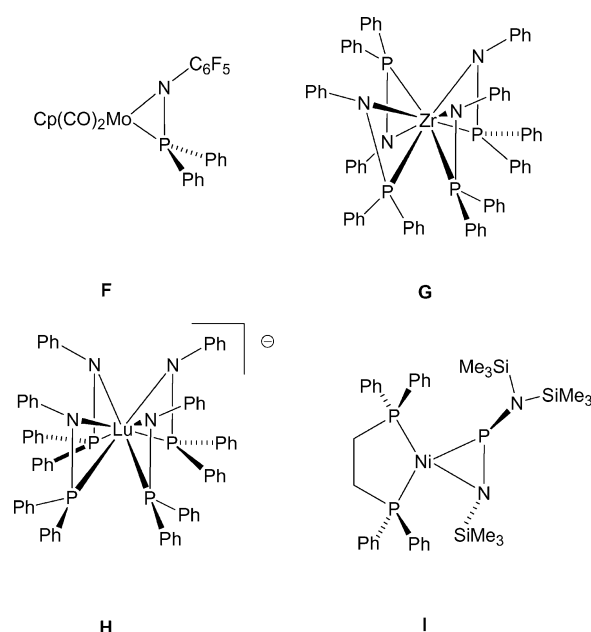


Chart 4

Nickel is both smaller and chemically softer than zirconium and the lanthanides, and a comparison of the title compounds with metalaazaphosphiranes of smaller and later transition metals is clearly more appropriate. Indeed, the metalaazaphosphirane moiety in the 18-electron complex $[(\eta^5-C_5H_5)(CO)_2Mo(Ph_2PNC_6F_5)]$, **F**, is closer to those of the title compounds.⁷ For example, the phosphorus–nitrogen bond is 1.640(3) Å long, while the molybdenum–phosphorus and molybdenum–nitrogen bonds are 2.362(2) and 2.239(3) Å long, respectively. But even if corrections are made for the approximately 0.15 Å larger covalent radius of molybdenum, *versus* nickel, the endocyclic bonds in **F** are still almost 0.1 Å longer.

To determine whether the very symmetrical bonding in the three-membered rings in **5**, **6**, **8**, **10** and **11** are mainly due to the metal or the uncommon ligand(s), it would of course have been best to compare our data to those of nickelaazaphosphiranes based on acyclic amidophosphines. Unfortunately the reaction of $[NiCl_2(PPh_3)_2]$ with $Li(PhNPPH_2)$ did not furnish a three-membered ring, but produced instead a dinuclear nickel–nickel bonded species with a bridging anionic $PhNPPH_2$ moiety.³⁴ A better structure match for the title compounds is the pseudo square-planar nickel complex **I**,³⁵ although here the nickelaazaphosphirane is composed of a nickel(0) center and a neutral amino(imino)phosphine ligand. Not unexpectedly, the three

bonds of this metalacycle, namely, Ni–P 2.231(1), Ni–N 1.908(2), P–N 1.646(2) Å, are somewhat different from those in the title complexes. Notably, it is the nickel–phosphorus bond of **I**, which shows the greatest discrepancy, being substantially longer than those in the title compounds. In addition, the phosphorus–nitrogen bond has lengthened significantly from 1.545(2) Å in the free iminophosphine to 1.674(1) Å in the complex. Because iminophosphines are valence-isoelectronic with alkenes, **I** may be considered a phosphorus–nitrogen analogue of a zerovalent nickel olefin complex.

The bonding in metalaazaphosphiranes

Three-membered rings are comparatively rare in main-group chemistry, because their substantial angle strain renders them unstable with respect to their acyclic analogues. Whenever such rings are encountered, however, they tend to contain nitrogen or phosphorus, or both elements. In transition-metal chemistry, by contrast, three-membered rings are much more common, although this is in part due to the ambiguity of assigning formal bonds in such compounds. The best-known examples of transition-metal-containing three-membered heterocycles are metalacyclopropanes, which are formed when alkenes coordinate to low-valent metal centers. To account for the bonding of these neutral ligands to the often neutral metal fragments, Dewar and Chatt proposed that the metal receives electron density from the π bond into an empty σ -type orbital, which is then synergistically back-donated from an occupied π -type d-orbital into the π^* orbital of the alkene.³⁶ This net electron flow from a bonding to an antibonding orbital is accompanied by a diagnostic carbon–carbon bond lengthening. For the bonding of the iminophosphine in **I** the Dewar–Chatt model is appropriate, as underscored by the substantial lengthening of the P=N bond upon coordination, although here back donation probably plays only a minor role.

Most amidophosphines are satisfactorily written as shown in **J** (Chart 5), and to account for the bonding of such an anion to transition metals it is not necessary to invoke the Dewar–Chatt model. Instead, the interaction of LX-type ligands with a metal is typically represented as shown in **K**, namely with a covalent bond from nitrogen and a donor bond from phosphorus. This mesomeric form describes the bonding for amidophosphines to lanthanides, main-group metals, and hard transition metals well, because it predicts metal–nitrogen and phosphorus–nitrogen single bonds and a (presumably weak) donor bond from phosphorus to the metal.

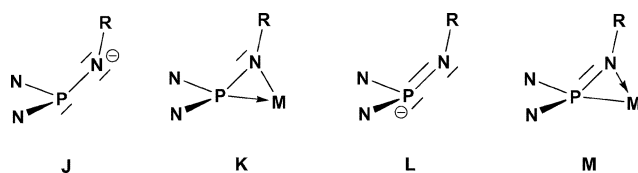


Chart 5

For late transition metals, and in particular for the title compounds, the resonance structure **K** neither describes the bonding pattern within the ligand nor the metal–ligand interaction properly, because it fails to account for the short nickel–phosphorus bond and the phosphorus–nitrogen double bond. The Dewar–Chatt model can also be discounted because the phosphorus–nitrogen bonds in the nickelaazaphosphiranes shorten, rather than lengthen, upon coordination.

The distinguishing features of the nickelaazaphosphiranes reported herein are the highly contracted phosphorus–nitrogen and phosphorus–nickel bonds; a bond pattern that is almost exactly opposite from that observed in all previously reported metalaazaphosphiranes. It thus appears that the amidophosphines based on heterocycles in their “free” anionic form are best represented as shown in **L**. This resonance structure, which

has been invoked previously and which also has theoretical support, places the negative charge on the more electropositive phosphorus atom.³³ The accumulation of negative charge and concomitant shielding of the phosphorus atoms is reflected in the significant upfield shifts of their signals in the ³¹P NMR spectra. There is also ample evidence, from reactivity and structural studies, that anionic amidophosphines act as P-centered anions.¹¹

In this context it is worth noting that phosphalkenes often exhibit a similar reversal of polarization with the negative charge residing on phosphorus, rather than carbon.³⁷ For amidophosphines, where such a charge reversal would seem less likely, it should be aided by electron-releasing groups on the amido nitrogen and electron withdrawing groups on the phosphorus atom and result in a formal phosphorus–nitrogen double bond. One would expect amidophosphines of this type to bind to metals as shown in **M**, namely with a covalent bond between the metal and phosphorus, a donor bond between the metal and the nitrogen atom and with a double bond between phosphorus and nitrogen. Our structural data bear this out, because the anionic P,N moieties of all seven nickelaazaphosphiranes reported here have double-bond lengths, while the nickel–phosphorus bonds, are among the shortest dozen such bonds reported.³² There are also inductive and resonance effects, which are both due to the aromatic ring, the inductive effects being evident in the longer P–N bonds of **10** and **11**, while the resonance effects are reflected in the significantly shortened N2–C6 and C1–C6 bonds of **11**.

In its limit the resonance form **L** may be expected to force the κ^2P coordination of a dianionic ligand like **9a**. Such κ^2P coordinations has been observed for the monoanionic bis(diphenylphosphino)amide [Ph₂PNPPh₂][−] where this bonding mode is favored over a $\kappa P,N$ coordination in most cases.¹¹ The partial realization of the κ^2P coordination mode in **11** suggests that, given a suitable linker and substituents, it should be possible to isolate metal complexes featuring chelating κ^2P -coordinated amidophosphines for ligands that are structurally more complex than [Ph₂PNPPh₂][−]. This will likely require a linker with a wider span than the *o*-phenylenediamine used in **9a**, namely an *m*-phenylenediamine, or an aliphatic linker of similar size. The role of the metal should be considered as well, and it stands to reason that soft metals which prefer phosphorus coordination in neutral aminophosphines, such as in **2**, should also favor the κP coordination of anionic amidophosphines.

Conclusion

The coordination chemistry of the PN moiety in its neutral and anionic form with nickel species was investigated. Neutral bis(*tert*-butylamino)diazadiphosphetidines coordinate nickel through phosphorus and thus shows a similar coordination behavior as trialkylphosphines. Anionic mono- and bis(amido)phosphines based on diazadiphosphetidines and related heterocycles, in contrast, bind nickel species in a much less predictable manner. Most commonly, these ligands coordinate nickel through both nitrogen and phosphorus simultaneously to yield remarkably stable three-membered Ni–P–N rings—nickelaazaphosphiranes. Unlike previously-studied metalaazaphosphiranes, these complexes feature strong bonds between both, nickel and nitrogen and nickel and phosphorus, and formal double-bonds between phosphorus and nitrogen. Our attempts to force a new chelating dianionic bis(amidophosphine) to bind nickel exclusively in a κ^2P fashion, succeeded only partially, leading to $\kappa P,N;\kappa P$ -bound ligands instead. When such anionic amidophosphines coordinate a metal through phosphorus alone, only the anionic model provides a correct electron count on the metal. In the hands of Peters *et al.* anionic phosphines have been remarkably useful in the elucidation of steric and electronic phenomena of late first-row transition metals, and amidophosphines, suitably modified, may prove to have similar utility.

Experimental

All operations were performed under an atmosphere of argon or pre-purified nitrogen on conventional Schlenk lines or in a glove box. The hydrocarbon or ethereal solvents were pre-dried over molecular sieves or CaH₂ and distilled under nitrogen from sodium or potassium immediately before use. *trans*-[NiCl₂(PEt₃)₂] and *trans*-[NiCl₂(PⁿBu₃)₂] were synthesized according to published procedures.¹⁵ {(Li·THF)(BuⁿN)P(μ-NBu^t)₂P(NBu^t)(Li·THF)},¹⁴ and Me₂Si(μ-NBu^t)₂PCl³⁸ were prepared as previously reported. The synthesis of {Me₂Si(μ-NBu^t)₂PN(H)Bu^t}, **7**, via a thermolysis reaction, had been reported previously;²⁶ a modified version appears below.

NMR spectra were recorded on Varian VXR-300 or Bruker Avance-500 spectrometers. ¹H, ¹³C, ³¹P and ²⁹Si NMR spectra are referenced relative to C₆D₆H (7.15 ppm), C₆H₆ (128.0 ppm), P(OEt)₃ (137.0 ppm) and TMS (0.0 ppm), respectively. Melting points were recorded on a Mel-Temp melting point apparatus; they are uncorrected. E & R Microanalytical Services, Parsippany, N. J. performed the elemental analyses.

Syntheses

trans-[{Bu^t(H)NP(μ-NBu^t)₂PN(H)Bu^t}₂NiCl₂]-C₆H₅CH₃ (**2**). In a 100 mL two-necked flask, anhydrous NiCl₂ (0.229 g, 1.77 mmol) and **1** (1.29 g, 3.90 mmol) were combined in toluene (25 mL). The initially orange suspension became dark-red during a 20 h reflux. The solution was filtered warm on a medium-porosity frit to remove metallic nickel and kept at 60 °C for 5 days, while dark red crystals formed (1.43 g, 87.9%). Mp 250 °C (decomp.). Found: C, 50.48; H, 10.19; N, 12.67. C₃₉H₈₄Cl₂N₈NiP₄ requires C, 50.99; H, 9.22; N, 12.20%. δ_H (C₆D₆) 1.939 (18 H, s), 1.283 (9 H, s), 1.194 (9 H, s); δ_C (C₆D₆) 54.42 (d), 53.55 (m), 51.58 (d, J_{PC} = 14.5 Hz), 33.45 (d, J_{PC} = 11.3 Hz), 33.03 (m, J_{PC} = 7.7 Hz), 32.27 (s); δ_P (C₆D₆) 71.76 (s); 30.13 (s).

cis-{Bu^t(H)NP(μ-NBu^t)₂POBu^t} (**4**). In a 100-mL two-neck flask, *cis*-[Bu^t(H)NP(μ-NBu^t)₂PCl] (0.27 g, 0.88 mmol) was dissolved in 15 mL hexanes, and the cooled (−78 °C) solution was treated with 0.88 mL of a 1.0 M LiOBu^t solution (hexanes). The mixture was allowed to warm to RT, then kept at 40 °C for 48 h, filtered on a medium-porosity frit and concentrated *in vacuo* to ca. 5 mL. After the solution had been stored in a freezer (−21 °C) for several days, colorless crystals formed. Yield: 0.27 g, 88%.

Mp 59–62 °C. Found: C, 55.07; H, 11.03; N, 11.81. C₁₆H₃₇N₃OP₂ requires C, 55.01; H, 10.60; N, 12.03%. δ_H (C₆D₆) 1.45 (18 H, s, NBu^t), 1.41 (9 H, s, NBu^t), 1.13 (9 H, s, OBu^t). δ_C (C₆D₆) 75.45 (d, J_{PC} = 8.5 Hz), 51.82 (t, J_{PC} = 12.4 Hz), 51.27 (s), 32.65 (d, J_{PC} = 9.5 Hz), 31.68 (d, J_{PC} = 10.1 Hz). δ_P (C₆D₆) 132.2 (s), 103.9 (s).

[{Bu^tOP(μ-NBu^t)₂PNBu^t}Ni(PBuⁿ)₃Cl] (**5**). A solution of the lithium salt of **4**, prepared by treating **4** (1.30 g, 3.72 mmol) with *n*-butyllithium (1.49 mL, 3.72 mmol), was added to a suspension of [NiCl₂(PⁿBu₃)₂] (1.35 g, 3.72 mmol) in hexanes (15 mL). The reaction mixture was refluxed overnight and the lithium chloride removed by filtration through a medium-porosity frit. After the solution had been allowed to cool, it was concentrated *in vacuo* to ca. 5 mL, and placed in a freezer (−21 °C) to afford several crops of well-developed orange-red crystals. Yield: 1.27 g, 53.6%.

Mp 176–179 °C. Found: C, 52.46; H, 9.96; N, 6.64. C₂₈H₆₃ClN₃NiOP₃ requires C, 52.15; H, 9.85; N, 6.52%. δ_H (C₆D₆) 1.626 (9 H, s), 1.592 (30 H, s), 1.349 (6 H, m, J_{HH} = 7.0 Hz), 1.200 (s, 9 H, NBu^t), 0.918 (9 H, t, J_{HH} = 7.4 Hz). δ_C (C₆D₆) 76.82 (d, J_{PC} = 8.8 Hz), 54.25 (d, J_{PC} = 27.5 Hz), 53.06 (dd, J_{PC} = 7.6, 3.1 Hz), 32.79 (d, J_{PC} = 4.1 Hz), 32.33 (t, J_{PC} = 5.6 Hz), 31.30 (d, J_{PC} = 8.8 Hz), 27.09 (s), 25.94 (dd, J_{PC} = 25.5, 1.7 Hz), 25.01 (d, J_{PC} = 12.9 Hz), 14.03 (s); δ_P (C₆D₆) 109.6 (d,

J_{PP} = 24.7 Hz), 15.2 (d, J_{PP} = 85.3 Hz), −53.6 (dd, J_{PP} = 84.2, 24.7 Hz).

[(PⁿBu₃)₃CINi{Bu^tNP(μ-NBu^t)₂PNBu^t}NiCl(PBuⁿ)₃] (**6**). *trans*-NiCl₂[PⁿBu₃]₂ (0.710 g, 1.33 mmol), dissolved in 10 mL of toluene, was treated dropwise with a toluene solution of {(Li·THF)(BuⁿN)P(μ-NBu^t)₂P(NBu^t)(Li·THF)} (0.746 g, 1.48 mmol) at RT. The resulting dark-red solution was kept at 50 °C for 16 h, filtered through a medium porosity frit, and concentrated *in vacuo* to a volume of ca. 15 mL. The solution was then kept at −12 °C to afford several crops of small, red-brown crystals. The yield was 0.332 g (53.1%), based on *trans*-[NiCl₂(PⁿBu₃)₂].

Mp 164 °C. Found: C, 51.29; H, 10.16; N, 5.97. C₄₀H₉₀Cl₂N₄Ni₂P₄ requires C, 51.15; H, 9.66; N, 5.96%. δ_H (C₆D₆) 1.88 (18 H, s, NBu^t), 1.67 (12 H, m, NBuⁿ), 1.52 (12 H, m, NBuⁿ), 1.46 (18 H, s, NBu^t), 1.35 (12 H, q, J_{HH} = 7.2 Hz, NBuⁿ), 0.89 (18 H, t, J_{HH} = 7.3 Hz, Buⁿ); δ_C (C₆D₆) 54.97 (s, NBu^t), 53.84 (t, J_{PC} = 14.1 Hz, NBu^t), 32.95 (s, NBu^t), 32.70 (t, J_{PC} = 4.6 Hz, NBu^t), 27.21 (s, Buⁿ), 25.05 (d, J_{PC} = 11.9 Hz, Buⁿ), 24.45 (d, J_{PC} = 25.0 Hz, Buⁿ), 14.12 (s, Buⁿ); δ_P (C₆D₆) 12.19 (dm, J_{PP} = 84.5 Hz), −82.43 (dt, J_{PP} = 85.4, 21.6 Hz).

Me₂Si(μ-NBu^t)₂PN(H)Bu^t (**7**). *n*-Butyllithium (16.2 mL, 40.5 mmol) was added dropwise to a toluene (25 mL) solution of *tert*-butylamine (4.25 mL, 40.4 mmol) at 0 °C, and the solution was refluxed for 1 h. In a separate flask, Me₂Si(μ-NBu^t)₂PCl (10.79 g, 40.4 mmol) was dissolved in 25 mL of toluene. This solution was cooled to 0 °C and treated dropwise with the lithium *tert*-butylamide solution. The ice-bath was removed and the mixture was stirred for 18 h at RT, during which time it turned a light tan color and a white precipitate formed. The mixture was filtered through a medium porosity frit and concentrated *in vacuo*. The brownish liquid was distilled under vacuum (46–49 °C, 0.1 mmHg) to give 9.66 g (78.7%) of a viscous colorless liquid. Bp 46–49 °C, 0.1 mmHg. δ_H (C₆H₆) 2.16 (1 H, d, J = 5.5 Hz, NH), 1.26 (18 H, d, J = 0.5 Hz, N^tBu), 1.25 (9 H, d, J = 1.3 Hz, NH^tBu), 0.37 (3 H, s, SiMe), 0.33 (s, 3 H, SiMe). δ_C (C₆H₆) 51.3 (d, J_{PC} = 12.9 Hz, NH(CMe₃)), 50.6 (d, J_{PC} = 10.4 Hz, N(CMe₃)), 33.3 (d, J_{PC} = 10.1 Hz, NH(CMe₃)), 33.1 (d, J_{PC} = 6.8 Hz, N(CMe₃)), 9.0 (d, J_{PC} = 2.6 Hz, SiMe), 5.8 (s, SiMe); δ_P (C₆H₆) 114.8 (s); δ_{Si} (C₆H₆) 5.1 (s).

[[Me₂Si(μ-NBu^t)₂PNBu^t}NiCl(PBuⁿ)₃] (**8**). A 100-mL two-necked flask, equipped with inlet, stirbar and funnel was charged with **7** (0.300 g, 0.988 mmol) and toluene (10 mL). The solution was treated dropwise with *n*-butyllithium (0.40 mL, 1.0 mmol) and refluxed (1 h). This solution was added dropwise at RT to a solution of [(Buⁿ)₃P]₂NiCl₂ (0.540 g, 1.01 mmol) in hexanes (10 mL) and the ensuing reaction mixture was refluxed for 16 h. The solution was then taken to dryness *in vacuo*, extracted with hexanes (20 mL) and the extract was filtered on a medium-porosity frit. The filtrate was concentrated *in vacuo* (10 mL) and stored in a freezer (−21 °C) until orange-brown crystals had formed (0.415 g, 70%). Mp 128 °C. Found: C, 52.55; H, 10.13; N, 6.96. C₂₆H₆₀ClN₃NiP₂Si requires C, 52.14; H, 10.10; N, 7.02%. δ_H (C₆D₆) 1.65 (6 H, m, CH₂), 1.59 (6 H, m, CH₂), 1.55 (9 H, s, NHBu^t), 1.45 (18 H, s, NHBu^t), 1.37 (6 H, m, CH₂), 0.90 (9 H, m), 0.20 (3 H, s, SiMe), 0.17 (3 H, s, SiMe); δ_C (C₆D₆) 52.9 (dd, J_{PC} = 28.8, 1.6 Hz), 51.9 (s, J_{PC} = 1.6 Hz), 33.0 (d, J_{PC} = 28.8, 5.8 Hz), 32.4 (dd, J_{PC} = 4.5, 1.5 Hz), 27.0 (s, CH₂), 25.3 (dd, J_{PC} = 24.2, 2.1 Hz, CH₂), 13.9 (s, Me), 3.7 (d, J_{PC} = 3.8 Hz, SiMe), 3.1 (d, J_{PC} = 7.1 Hz, SiMe); δ_P (C₆D₆) 14.1 (d, J_{PP} = 80.2 Hz), −53.9 (d, J_{PP} = 80.2 Hz); δ_{Si} (C₆D₆) −1.4 (s).

1,2-{Me₂Si(μ-NBu^t)₂PNH}₂C₆H₄ (**9a**). In a 100 mL two-necked flask, 1,2-diaminobenzene (1.1 g, 10 mmol), dissolved in THF (20 mL), was treated with *n*-butyllithium (8.5 mL, 21 mmol) at RT. After the completion of the addition, the solution was refluxed for 2 h while it became deep blue. In a 250-mL flask, equipped with a dropping funnel, Me₂Si(μ-NBu^t)₂PCl (5.6 g, 21 mmol) was dissolved in toluene (100 mL) and then

treated dropwise with the dilithio salt. The reaction mixture was stirred overnight and the solvents were removed *in vacuo*. The remaining solid was redissolved in toluene (40 mL) and the ensuing extract was filtered on a medium-porosity frit and concentrated to *ca.* 15 mL *in vacuo*. It was stored for several days at $-17\text{ }^{\circ}\text{C}$ to produce colorless crystals (5.2 g, 86%). Mp 186–188 $^{\circ}\text{C}$ Found: C, 54.90; H, 9.70; N, 14.74. $\text{C}_{26}\text{H}_{54}\text{N}_6\text{P}_2\text{Si}_2$ requires C, 54.90; H, 9.57; N, 14.77%. δ_{H} (C_6D_6) 7.57 (2 H, m, Ph), 6.86 (2 H, m), 4.65 (2 H, s, NH), 1.22 (18 H, s, Bu¹), 0.44 (6 H, s, Me), 0.37 (6 H, s, Me); δ_{C} (C_6D_6) 134.2 (d, $J_{\text{PC}} = 7.8$ Hz), 121.1 (s), 119.26 (d, $J_{\text{PC}} = 17.6$ Hz), 50.51 (d, $J_{\text{PC}} = 10.4$ Hz), 32.96 (d, $J_{\text{PC}} = 6.8$ Hz), 8.85 (d, $J_{\text{PC}} = 1.8$ Hz), 5.34 (s); δ_{P} (C_6D_6) 119.16 (s); δ_{Si} (C_6D_6) 10.13 (s).

1-[Me₂Si(μ-NBu¹)₂P]₂N-2-NH₂(C₆H₄) (9b). In a 250 mL two-necked flask, 1,2-diaminobenzene (3.94, 36.4 mmol), dissolved in THF (50 mL), was treated with *n*-butyllithium (30 mL, 72 mmol) at RT. Upon completion of the addition, the solution was refluxed for 2 h, during which time it became deep-blue. The solution was then treated dropwise at RT with a solution of Me₂Si(μ-NBu¹)₂PCl (19.4 g, 72.8 mmol), dissolved in toluene (50 mL). The reaction mixture was stirred overnight and the solvents were removed *in vacuo*. The remaining solid was extracted with hexanes (40 mL), and the ensuing extract was filtered on a medium-porosity frit and concentrated to *ca.* 15 mL *in vacuo* to yield **9a** and **9b** in a 3 : 1 ratio by NMR. After storing the solution at $-17\text{ }^{\circ}\text{C}$ a crop of colorless, trapezoidal crystals of **9b** was isolated (5.3 g, 25%). Further cooling of the supernatant afforded **9a** (9.3 g, 44%). Mp 166–170 $^{\circ}\text{C}$. δ_{H} (C_6D_6) 7.74 (1 H, d, $J_{\text{HH}} = 7.5$ Hz), 6.94 (1 H, t, $J_{\text{HH}} = 7.5$ Hz), 6.71 (1 H, t, $J_{\text{HH}} = 7.8$ Hz), 6.50 (1 H, d, $J_{\text{HH}} = 7.8$ Hz Ph), 4.89 (2 H, s, NH₂), 1.31 (18 H, s, Bu¹), 1.27 (18 H, s, Bu¹), 0.40 (6 H, Me), 0.35 (6 H, Me); δ_{C} (C_6D_6) 145.2 (s), 131.6 (t, $J_{\text{HH}} = 2.9$ Hz), 129.5 (t, $J_{\text{HH}} = 6.2$ Hz), 125.3 (s), 116.0 (s), 114.8 (s), 51.6 (t, $J_{\text{PC}} = 5.8$ Hz), 51.4 (t, $J_{\text{PC}} = 6.2$ Hz), 33.2 (t, $J_{\text{HH}} = 3.7$ Hz) 32.8 (t, $J_{\text{PC}} = 3.8$ Hz), 8.1 (s), 7.4 (s); δ_{P} (C_6D_6) 141.7 (s); δ_{Si} (C_6D_6) 8.1 (s).

[1-[Me₂Si(μ-NBu¹)₂PN]-2-[Me₂Si(μ-NBu¹)₂PNH]C₆H₄NiCl] (10). A sample of **9a** (0.555 g, 0.976 mmol) was dissolved in THF (15 mL) and the ensuing solution was treated with *n*-butyllithium (2.0 mmol). The mixture was refluxed for 2 h, allowed to cool to RT and then added dropwise to a suspension of NiCl₂ (0.128 g, 0.987 mmol) in THF (10 mL). After it had been stirred for a few minutes, the initially colorless mixture turned green and after 12 h of refluxing, it became maroon. The THF was removed *in vacuo* and the residue was extracted with toluene (30 mL), filtered and concentrated *in vacuo* to *ca.* 15 mL. After the solution had been stored at $-22\text{ }^{\circ}\text{C}$ for several days, rod-shaped, maroon crystals (0.508 g) formed. Yield: 76.7%. Mp 226–228 $^{\circ}\text{C}$. Found: C, 52.60; H, 8.18; N, 11.32. $\text{C}_{33}\text{H}_{61}\text{ClN}_6\text{NiP}_2\text{Si}_2$ requires C, 52.56; H, 8.15; N, 11.14%. δ_{H} (C_6D_6) 7.19 (2 H, d, $J_{\text{HH}} = 7.8$ Hz); 6.79 (1 H, t, $J_{\text{HH}} = 7.7$ Hz), 6.63 (1 H, t, $J_{\text{HH}} = 7.6$ Hz), 6.72 (2 H, d, $J_{\text{HH}} = 7.3$ Hz), 6.08 (1 H, d, $J_{\text{HH}} = 7.9$ Hz), 4.09 (1 H, t, $J_{\text{PH}} = 8.7$ Hz), 1.62 (18 H, s, NBu¹), 1.45 (18 H, s, NBu¹), 0.63 (3 H, s, Me), 0.30 (6 H, d, $J_{\text{PH}} = 1.5$ Hz, Me), 0.20 (3 H, s, Me); δ_{C} (C_6D_6) 137.8 (s), 132.6 (d, $J_{\text{PC}} = 8.7$ Hz), 125.6 (s), 121.2 (d, $J_{\text{PC}} = 11.6$ Hz), 120.0 (s), 119.0 (s), 51.8 (d, $J_{\text{PC}} = 3.7$ Hz), 51.7 (d, $J_{\text{PC}} = 4.9$ Hz), 33.5 (d, $J_{\text{PC}} = 29.4$ Hz), 32.2 (d, $J_{\text{PC}} = 6.1$ Hz), 6.1 (s), 3.9 (m), 3.8 (d, $J_{\text{PC}} = 3.0$ Hz), 3.6 (d, $J_{\text{PC}} = 3.0$ Hz); δ_{P} (C_6D_6) 94.7 (d, $J_{\text{PP}} = 667$ Hz), -28.3 (d, $J_{\text{PP}} = 667$ Hz); δ_{Si} (C_6D_6) 13.8 (s), 8.7 (s).

[1,2-[Me₂Si(μ-NBu¹)₂PN]₂]{Me₂Si(μ-NBu¹)₂PN}C₆H₄Ni{PEt₃} (11). To a 100 mL two-necked flask, equipped with a stir bar and dropping funnel was added **9a** (0.508 g, 0.900 mmol) and hexanes (10 mL). The ensuing solution was treated with *n*-butyllithium (1.80 mmol) and refluxed for 2 h. It was then added dropwise at RT to a hexanes (10 mL) solution of *trans*-[NiCl₂(PEt₃)₂] (0.328 g, 0.900 mmol). The initially red mixture was refluxed for 12 h, during which time it turned green–brown. After the solution had cooled to RT, it was filtered

to remove LiCl, concentrated *in vacuo* and stored at $-21\text{ }^{\circ}\text{C}$ to afford a dark green (almost black) solid (0.617 g, 82.1%). Mp 98–101 $^{\circ}\text{C}$. Found: C, 52.07; H, 9.21; N, 10.86. $\text{C}_{32}\text{H}_{67}\text{N}_6\text{NiP}_3\text{Si}_2$ requires C, 51.68; H, 9.08; N, 11.30%. δ_{H} (C_6D_6) 7.52 (2 H, m, $J_{\text{HH}} = 7.8$ Hz), 7.09 (1 H, m, Ph), 6.86 (2 H, m, Ph), 1.69 (6 H, t, $J_{\text{PH}} = 7.8$ Hz), 1.50 (18 H, s, NBu¹), 1.25 (18 H, s, NBu¹), 0.96 (9 H, m), 0.68 (3 H, s, Me), 0.47 (6 H, s, Me); δ_{C} (C_6D_6) 146.8 (d, $J_{\text{PC}} = 8.7$ Hz), 125.0 (d, $J_{\text{PC}} = 18.6$ Hz), 121.7 (s), 117.9 (s), 115.3 (t, $J_{\text{PC}} = 19.8$ Hz), 114.4 (s), 52.0 (d, $J_{\text{PC}} = 15.1$ Hz), 51.3 (d, $J_{\text{PC}} = 3.7$ Hz), 33.4 (d, $J_{\text{PC}} = 6.1$ Hz), 32.5 (d, $J_{\text{PC}} = 5.8$ Hz), 17.8 (dd, $J_{\text{PC}} = 8.4$, 24.7 Hz), 7.99 (m), 7.35 (t, $J_{\text{PC}} = 6.3$ Hz), 4.56 (d, $J_{\text{PC}} = 3.9$ Hz), 4.31 (d, $J_{\text{PC}} = 6.7$ Hz), 3.96 (m); δ_{P} (C_6D_6) 78.1 (dd, $J_{\text{PP}} = 413.9$, 39.3 Hz), 20.5 (m), -6.3 (dd, $J_{\text{PP}} = 413.8$, 70.0 Hz); δ_{Si} (C_6D_6) 7.7 (s), 1.7 (s).

X-Ray crystallography

Compounds 2, 3 and 8. All crystals were grown from supersaturated solutions at the indicated temperatures. Suitable, single crystals were coated with oil, affixed to a glass capillary, and centered on the diffractometer in a stream of cold nitrogen. Reflection intensities were collected with a Bruker SMART CCD diffractometer, equipped with an LT-2 low-temperature apparatus, operating at 213 K. Data were measured using ω scans of 0.3° per frame for 30 s until a complete hemisphere had been collected. The first 50 frames were recollected at the end of the data collection to monitor for decay. Cell parameters were retrieved using SMART³⁹ software and refined with SAINT⁴⁰ on all observed reflections. Data were reduced with SAINT, which corrects for Lorentz and polarization effects and decay. An empirical absorption correction was applied with SADABS.⁴¹ The structures were solved by direct methods with the SHELXS-90⁴² program and refined by full-matrix least squares methods on F^2 with SHELXL-97,⁴³ incorporated in SHELXTL Version 5.10.⁴⁴

Compounds 9a, 9b and 10. The crystals were sealed inside argon-filled glass capillaries, and the intensity data were collected on a Bruker P4 diffractometer. Three reflections were monitored after every 97 reflections, and the appropriate intensity corrections were applied during data reduction. Reflection data were reduced with XDISK of the SHELXTL-PC program suite, Version 4.1,⁴⁵ and the structure was solved by direct-methods with SHELXL-NT, Version 5.10,⁴⁶ and refined as described above.

Compound 11. Crystal data were collected at 100 K on a Bruker Smart Apex CCD instrument, using graphite-monochromated Mo-K α radiation ($\lambda = 0.71069\text{ \AA}$). The structure was solved with Direct Methods and refined by full-matrix least squares against F^2 using the SHELXTL, Version 5.10, program.

CCDC reference numbers 272420–272426.

See <http://dx.doi.org/10.1039/b507040f> for crystallographic data in CIF or other electronic format.

Acknowledgements

We thank the Chevron Phillips Chemical Company for Research Assistantships to I. S. and L. G., and the National Science Foundation for a GAANN fellowship to G. R. L.

References

- D. E. C. Corbridge, *Phosphorus*, Elsevier, Amsterdam, 5th edn, 1995.
- M. T. Ashby and Z. Li, *Inorg. Chem.*, 1992, **31**, 1321.
- Z. Fei, R. Scopelliti and P. J. Dyson, *Inorg. Chem.*, 2003, **42**, 2125; Z. Fei, R. Scopelliti and P. J. Dyson, *Dalton Trans.*, 2003, 2772; Z. Fei, R. Scopelliti and P. J. Dyson, *Eur. J. Inorg. Chem.*, 2004, 530; L. E. Anagho, J. F. Bickley, A. Steiner and L. Stahl, *Angew. Chem., Int. Ed.*, 2005, **44**, 3271.

- 4 O. Kühn, T. Koch, F. B. Somoza, Jr., P. C. Junk, E. Hey-Hawkins, D. Plat and M. Eisen, *J. Organomet. Chem.*, 2000, **604**, 116.
- 5 H. Schmidbaur, S. Lauteschläger and B. Milewski-Mahrla, *J. Organomet. Chem.*, 1983, **254**, 59.
- 6 J. Ellermann, J. Sutter, F. A. Knoch and M. Moll, *Angew. Chem., Int. Ed. Engl.*, 1993, **32**, 700; J. Ellermann, J. Sutter, C. Schelle, F. A. Knoch and M. Moll, *Z. Anorg. Allg. Chem.*, 1993, **619**, 2006; A. Winkler, W. Bauer, F. W. Heinemann, V. Garcia-Montalvo, M. Moll and J. Ellermann, *Eur. J. Inorg. Chem.*, 1988, 437; J. Ellermann, W. Bauer, M. Schutz, F. W. Heinemann and M. Moll, *Monatsh. Chem.*, 1998, **129**, 547.
- 7 E. Lindner, M. Heckmann, R. Fawzi and W. Hiller, *Chem. Ber.*, 1991, **124**, 2171.
- 8 T. G. Wetzel, S. Dehnen and P. W. Roesky, *Angew. Chem., Int. Ed.*, 1999, **38**, 1086.
- 9 R. R. Holmes and J. A. Forstner, *Inorg. Chem.*, 1963, **2**, 380.
- 10 J. C. T. R. Burckett St. Laurent, P. B. Hitchcock and J. F. Nixon, *J. Organomet. Chem.*, 1983, **249**, 243.
- 11 V. S. Reddy, S. S. Krishnamurthy and M. Nethaji, *J. Chem. Soc., Dalton Trans.*, 1994, 2661; V. S. Reddy, S. S. Krishnamurthy and M. Nethaji, *J. Chem. Soc., Dalton Trans.*, 1995, 1993.
- 12 H. J. Chen, A. Tarassoli, R. C. Haltiwanger, V. S. Allured and A. D. Norman, *Inorg. Chim. Acta*, 1982, **65**, L69.
- 13 N. Kuhn and M. Winter, *J. Organomet. Chem.*, 1983, **243**, C47; N. Kuhn and M. Winter, *J. Organomet. Chem.*, 1983, **243**, C42.
- 14 I. Schranz, L. Stahl and R. J. Staples, *Inorg. Chem.*, 1998, **37**, 1493.
- 15 K. A. Jensen, *Z. Anorg. Allg. Chem.*, 1936, **229**, 265.
- 16 V. Scatturin and A. Turco, *J. Inorg. Nucl. Chem.*, 1958, **8**, 447.
- 17 G. Linti, H. Nöth, E. Schneider and W. Storch, *Chem. Ber.*, 1993, **126**, 619.
- 18 L. Grocholl, L. Stahl and R. J. Staples, *Chem. Commun.*, 1997, 1465; D. F. Moser, I. Schranz, M. C. Gerrety, L. Stahl and R. J. Staples, *J. Chem. Soc., Dalton Trans.*, 1999, 751.
- 19 J. K. Brask, T. Chivers, M. L. Krahn and M. Parvez, *Inorg. Chem.*, 1998, **38**, 290; G. G. Briand, T. Chivers and M. Krahn, *Coord. Chem. Rev.*, 2002, **233–234**, 237.
- 20 K. V. Axenov, V. V. Kotov, M. Klinga, M. Leskelä and T. Reppo, *Eur. J. Inorg. Chem.*, 2004, 695; K. V. Axenov, M. Klinga, M. Leskelä, V. V. Kotov and T. Reppo, *Eur. J. Inorg. Chem.*, 2004, 4702.
- 21 W. Deissig and H. Dietrich, *Acta Crystallogr., Sect. B*, 1968, **24**, 108.
- 22 J. Koch, I. Hyla-Kryspin, R. Gleiter, T. Klettke and D. Walther, *Organometallics*, 1999, **18**, 4942.
- 23 C. E. MacBeth, J. C. Thomas, T. A. Betley and J. C. Peters, *Inorg. Chem.*, 2004, **43**, 4645; H. Schäfer, D. Binder and D. Fenske, *Angew. Chem., Int. Ed. Engl.*, 1985, **24**, 522; M. Aresta, C. F. Nobile, V. C. Albano, E. Forni and M. Manaserro, *J. Chem. Soc., Chem. Commun.*, 1975, 636.
- 24 We define symmetrical M–P and M–N bonds to mean that both bonds have normal bond lengths.
- 25 G. R. Lief, C. J. Carrow, L. Stahl and R. J. Staples, *Chem. Commun.*, 2001, 1562.
- 26 O. J. Scherer, M. Püttmann, C. Krüger and G. Wolmershäuser, *Chem. Ber.*, 1982, **115**, 2076.
- 27 T. Q. Ly, A. M. Z. Slawin and J. D. Woollins, *J. Chem. Soc., Dalton Trans.*, 1997, 1611; P. A. Bella, O. Crespo, E. J. Fernández, A. K. Fischer, P. G. Jones, A. Laguna, J. M. López-de-Luzuriaga and M. Monge, *J. Chem. Soc., Dalton Trans.*, 1999, 4009.
- 28 F. Garcia, R. A. Kowenicki, I. Kuzu, L. Riera, M. McPartlin and D. S. Wright, *Dalton Trans.*, 2004, 2904.
- 29 J. C. Thomas and J. C. Peters, *Inorg. Chem.*, 2003, **42**, 5055; T. A. Betley and J. C. Peters, *Inorg. Chem.*, 2003, **42**, 5074; T. A. Betley and J. C. Peters, *Angew. Chem., Int. Ed.*, 2003, **42**, 2385; C. E. MacBeth, J. C. Thomas, T. A. Betley and J. C. Peters, *Inorg. Chem.*, 2004, **43**, 4645; T. A. Betley and J. C. Peters, *J. Am. Chem. Soc.*, 2004, **126**, 6252.
- 30 R. H. Crabtree, *The Organometallic Chemistry of the Transition Metals*, Wiley, New York, 3rd edn, 2001, p. 92.
- 31 D. J. Mindiola and G. L. Hillhouse, *J. Am. Chem. Soc.*, 2001, **123**, 4623, and references cited therein.
- 32 Based on a CSD (version 5.26, November 2004) search of 1703 such compounds.
- 33 G. Trinquier and M. T. Ashby, *Inorg. Chem.*, 1994, **33**, 1306; W. W. Schoeller, T. Busch and E. Niecke, *Chem. Ber.*, 1990, **123**, 272; W. W. Schoeller, in *Multiple Bonds and Low Coordination in Phosphorus*, ed. M. Regitz and O. J. Scherer, Thieme, Stuttgart, 1990, pp. 5–32.
- 34 D. Fenske, B. Maczek and K. Maczek, *Z. Anorg. Allg. Chem.*, 1997, **623**, 1113.
- 35 O. J. Scherer, R. Walter and W. S. Sheldrick, *Angew. Chem., Int. Ed. Engl.*, 1985, **24**, 525.
- 36 M. J. S. Dewar, *Bull. Soc. Chim. Fr.*, 1951, C71–79; J. Chatt and L. A. Duncanson, *J. Chem. Soc.*, 1953, 2939.
- 37 L. Weber, *Eur. J. Inorg. Chem.*, 2000, 2425.
- 38 M. Veith, M. Grosser and V. Huch, *Z. Anorg. Allg. Chem.*, 1984, **513**, 89.
- 39 *SMART V 4.043 Software for the CCD Detector System*, Bruker Analytical X-ray Systems, Madison, WI, 1995.
- 40 *SAIN T V 4.035 Software for the CCD Detector System*, Bruker Analytical X-ray Systems, Madison, WI, 1995.
- 41 *SADABS program for absorption corrections using the Bruker CCD Detector System*, Based on: R. Blessing, *Acta Crystallogr., Sect. A*, 1995, **51**, 33.
- 42 G. M. Sheldrick, *SHELXS-90, Program for the Solution of Crystal Structures*, University of Göttingen, Göttingen, Germany, 1990.
- 43 G. M. Sheldrick, *SHELXL-97, Program for the Solution of Crystal Structures*, University of Göttingen, Göttingen, Germany, 1997.
- 44 *SMART Version 4.043 Software for the CCD Detector System*, Bruker Analytical X-ray Systems, Madison, WI, 1995.
- 45 *SHELXTL 5.10 (PC-Version)*, Siemens Analytical X-Ray Instruments, Inc., Madison, WI, 1998.
- 46 *SHELXTL NT Version 5.10, Program Library for Structure Solution and Molecular Graphics*, Bruker Analytical X-ray Systems, Madison, WI, 1999.